

Electrodeposition of Chitosan on Ti-6Al-4V Surfaces: A Study of Process Parameters

Marco León^a , Doménica Alvarez^a, Alfredo Valarezo^a, M. Lorena Bejarano^a, Daniela Viteri^b,

Astrid L. Giraldo-Betancur^c , Juan Muñoz-Saldaña^d, Jose Alvarez-Barreto^{b*} 

^aUniversidad San Francisco de Quito, Instituto de Investigación de Materiales, Departamento de Ingeniería Mecánica, Quito, Ecuador.

^bUniversidad San Francisco de Quito, Departamento de Ingeniería Química, Laboratorio de Biomateriales, Quito, Ecuador.

^cCONACYT-Centro de Investigación y de Estudios Avanzados del IPN, Querétaro, México.

^dCentro de Investigación y de Estudios Avanzados del IPN, Laboratorio Nacional de Proyección Térmica, CENAPROT Lib. Norponiente 2000, Fracc. Real de Juriquilla, 76230 Querétaro, Qro. México.

Received: October 22, 2021; Revised: February 01, 2022; Accepted: February 21, 2022

The effect of different electrodeposition variables of chitosan coatings on Ti-6Al-4V substrates is studied. Electrolytic solutions containing chitosan at 0.1, 0.5, and 1.0 wt/v% was used to coat Ti-6Al-4V grit-blasted samples through electrodeposition, at 1.5 and 3.0 V, for 2.5, 20 and 30 min. Coating surface morphology was analyzed by scanning electron microscopy. Adhesion behavior was characterized by scratch testing, and coating stability under physiological conditions was assessed by swelling test. Electrodeposited coatings with longer times and high chitosan concentrations produced porous coatings, with a hydrogel-like structure, with better surface adhesion than those at lower concentrations and times. Swelling tests displayed a high initial swelling with posterior rapid degradation and stabilization at 3h, indicating the potential need for a crosslinking agent. These results suggest that chitosan electrodeposition has great potential for coating applications of metallic implants, and further *in vitro* cell assays are proposed for future studies.

Keywords: Bioactive coatings, metallic implants, electrochemical deposition, chitosan, hydrogel.

1. Introduction

Metal implants as bone-anchored prostheses have been employed since 1965 for dental treatments, and today they are also used in orthopedic applications^{1,2}. This type of prosthesis offers multiple benefits that can be summarized in a better body image, comfort, and better mobility of the affected zone³. However, some problems arise in their use, especially when the prosthesis interacts with bone and is subjected to important mechanical loads. Infections, peri-prosthetic bone fracture, device breakage, and implant loosening are among the most common complications related to prostheses^{4,6}. Infections are reported in 73% of the cases, while peri-prosthetic bone fracture in 60%, device breakage in 53%, and implant loosening in 60%³. These problems are produced by many causes, but most importantly, a poor integration between bone and the metal surface seems to be the main source of difficulties^{4,7,8}. Thus, it is imperative to enhance prostheses osseointegration to reduce post-operative complications, and thereby, improve overall people's quality of life.

Certain parameters must be considered to tackle this problem. Topography, chemistry, and wettability of the prosthesis surface play an important role in the bone-metal bond⁹. Surfaces can be modified and adapted to improve osseointegration. Bioactive organic and inorganic coatings on prostheses have been widely investigated and represent a good alternative to enhance osseointegration^{10,11}. One of

those, that has gained considerable attention, is the use of biopolymers. Chitosan (CS) has been studied as a potential biopolymeric coating for application on metal prostheses, especially on titanium alloys¹². This polysaccharide, obtained by chitin de-acetylation, has suitable properties for the application, including biocompatibility, biodegradability, antibacterial and wound healing activity, and non-significant toxicity. Additionally, CS-coated surfaces support cell adhesion, proliferation and differentiation at the bone tissue-implant interphase, which is fundamental in the process of osseointegration¹³.

Several techniques have been previously employed to deposit CS coatings on implants, including solvent casting, immersion coating (simple absorption), layer-by-layer deposition, electrochemical methods, and electrophoretic deposition¹⁴⁻¹⁸. Electrodeposition techniques have great advantages compared to other methods due to the higher deposition speed, shorter processing time, and the possibility of controlling film thickness. Furthermore, complex shapes can be uniformly coated by electrodeposition, as well as on selected specific areas of the substrate^{19,20}. CS electrodeposition has been applied onto titanium surfaces (both as pure Ti and Ti-6Al-4V) in combination with different bioactive molecules, such as antibiotics, hydroxyapatite and other biopolymers²¹⁻²³. Results from these studies have shown stable coatings with important antibacterial activity, and the ability to support cell proliferation and differentiation. However, the assessment of different important electrodeposition parameters, such as time,

*e-mail: jalvarezb@usfq.edu.ec

voltage and CS concentration, has not been carried out on these surfaces. The electrodeposition of CS on gold surfaces have demonstrated that these variables have significant implications in coating thickness and morphology^{24,25}. Moreover, to our knowledge, there are no reports on the adhesion assessment of the electrodeposited CS to the metallic surface, nor has it been found any data on coating's pore size, and, in turn, the relationship with electrodeposition process parameters.

Consequently, the aim of this work was to analyze the effects of chitosan concentration, time and voltage on the chitosan electrodeposition process onto Ti-6Al-4V surfaces, particularly coating's morphology and adhesion behavior. Experimental data on deposition, coating thickness, microstructure, adhesion, and swelling tests are presented, including variations in dependence of the mentioned variables.

2. Experimental

2.1. Chitosan preparation

Chitosan with a medium molecular weight (800 KDa) and 98% deacetylation degree was used (Sigma-Aldrich, Catalog Number 448877). Solutions of chitosan at 0.1, 0.5 and 1.0 wt/v% CS were prepared in 1 v/v% acetic acid, and the pH was corrected to 5.5. Subsequently, the solutions were filtered and stored at 4 °C until use.

2.2. Surface preparation

Cylindrical samples of Ti-6Al-4V with a diameter of 6.7 mm and a thickness of 2.5 mm were used for electrodeposition. The discs were gritblasted with aluminum oxide particles in a pressure blast cabinet (BNP Double 220) with a distance of 0.1 m between the nozzle and the sample surface, and air pressure of 0.3 MPa²⁶. The Ra-roughness obtained was 3.13 μm for all samples. Prior to the CS electrodeposition, samples were cleaned with 70% ethanol in a BRANSON 1800 ultrasound device for 15 min.

2.3. Adsorption coating

A group of reference samples were coated through adsorption by introducing them in a 1.0 wt/v% chitosan

solution for 20, and 30 min at 25 °C. After coating, the samples were rinsed, frozen and lyophilized for further analyses.

2.4. Electrodeposition

Chitosan coating electrodeposition was performed at room temperature with an Agilent E3634A DC Power Supply with a digital multimeter by applying voltages of 1.5 and 3.0 V. Time periods and voltages are presented in Table 1. A copper disc (6.7 mm diameter and 5.0 mm thick) was used as the anodic electrode and the Ti-6Al-4V disc as the working electrode.

Three different solutions with chitosan concentrations of 0.1, 0.5, and 1.0 wt/v% at a pH of 5.5 were used. All samples were frozen and lyophilized prior to morphology analyses.

In Figure 1, a diagram of the electrolytic cell used in this study is represented. Ti-6Al-4V and Cu appear submerged in the chitosan solution as cathode and anode electrode, respectively.

2.5. Morphology and thickness analyses

Surface morphology was examined by scanning electron microscopy, SEM- JEOL JSM-IT300, at 5-20kV and 50 Pa. For thickness measurements, samples were embedded in an epoxy resin (EpoThin™ 2, Buehler), and cross-sections were produced by cutting the chitosan-coated Ti-6Al-4V with a diamond blade. The cutting was performed transversally to the coating, at different time intervals, at a cutting speed of 500 rpm and feed rate of 0.15 mm/min to not affect the deposited chitosan layer. Energy-dispersive X-ray spectroscopy (EDS) was performed on sample cross-sections to analyze CS presence and measure coating thickness. Pore size and coating thickness were determined with SEM images by

Table 1. Electrodeposition variables to deposit chitosan over Ti-6Al-4V substrates.

Voltage (V)	Time (min)	Chitosan Concentrations (wt/v%)
1.5	2.5	0.1 0.5 1
3.0	20	0.1 0.5 1
	30	

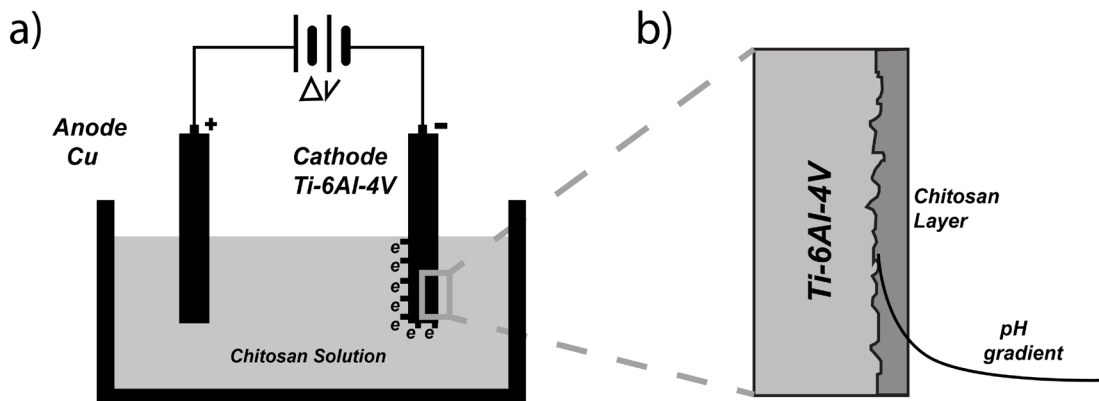


Figure 1. Electrodeposition process: a) Chitosan electrodeposition on Ti-6Al-4V surface, b) Coated layer of chitosan on grit blasted surface of Ti-6Al-4V and pH gradient on the cathode.

processing them in the software ImageJ. Three samples were analyzed for each condition, and the mean size \pm standard deviation and the pore size distribution were obtained.

2.6. FTIR Analysis

Native and electrodeposited chitosan samples were analyzed in a Fourier transformed infrared spectrometer; model Cary 630 FTIR-ATR (Agilent Technologies), in the region between 500 and 4000 cm^{-1} .

2.7. Scratch test

The adhesion of the different coatings was studied through the scratch test. The test was performed using a Rockwell AJ-227 Scratch Tester, with a 200- μm radius diamond tip. A normal force was applied on the surface at a constant rate of increase as the indenter moved 3.5 μm distance with a velocity of 10 mm/min. The applied load was increased progressively from 0 to 35 N. Three scratches, separated by at least 1 mm, were created on each type of sample, in at least two specimens. Normal and tangential forces were measured through each scratching path. With these forces, the coefficient of friction of each coating was calculated to assess the adhesion to the substrate. Additionally, a substrate without chitosan coating was used as a blank.

2.8. Swelling test

The ability of the chitosan coatings to absorb water was evaluated with the swelling test as a way of estimating coating stability under physiological conditions. Three samples for each condition were initially weighed and later immersed in 5 ml of phosphate buffered saline (PBS, pH 7.4) at 37 $^{\circ}\text{C}$. The weight of each test sample was measured at different times: 0, 0.25, 0.5, 1, 2, 3, and 24 hours. Swelling degree was calculated through Equation 1.

$$\%SD = (w_o - w_i) / w_i \times 100 \quad (1)$$

Where, % SD corresponds to the swelling degree, and w_o and w_i to the weight of the tested samples before and after immersing into PBS, respectively. Swelling degree was reported as the (average \pm standard deviation) and plotted against time. Significant differences were determined through ANOVA and Tukey pair-wise comparison, with a 95% confidence level.

3. Results and Discussion

3.1. Electrodeposition of chitosan on Ti-6Al-4V

CS is a stimuli-responsive and film-forming biopolymer, and, because of this, it has been used for metallic implant coatings to improve osseointegration²⁷. Electrodeposition, on the other hand, is one of the methods used to deposit chitosan on metal surfaces; however, generally, unlike in the present study, CS is electrodeposited with co-factors, such as other polymers, nanostructures, biomolecules, or dyes, among others²⁸⁻³¹. The mechanism of CS electrodeposition is the dehydrogenation (or deprotonation) of the backbone that allows the formation of a film³².

By applying a current density near to the cathode electrode, redox reactions take place. The electrons of the cathode react with the CS in solution and produce hydroxide ions

that increase the pH. The primary amines of the chitosan are deprotonated, forming an insoluble hydrogel film on the substrate^{33,34}. It is well known that CS forms an insoluble film on Ti-6Al-4V under high pH values over 5-6, while under low pH values, chitosan is soluble and remains in solution^{32,35}. Thus, in the present study, the effect of different electrodeposition conditions, particularly voltage, chitosan concentration, and time, was assessed to use this technique in future applications of implant coatings.

In order to assess possible changes in CS molecular structure due to electrodeposition, an FTIR analysis was carried out on native chitosan and 1.0% CS- 30 min coating, and the spectra are shown in Figure 2. Characteristic CS peaks were observed around 1580 cm^{-1} due to $-\text{NH}_2$ stretching, while $\text{C}=\text{O}$ vibrations were present at 1140 cm^{-1} . Peaks at 1020 and 1140 cm^{-1} are attributed to symmetric and asymmetric $\text{C}-\text{O}-\text{C}$ vibrations³⁶. These peaks were maintained in both samples, implying that electrodeposition did not significantly alter the CS backbone molecular structure. A similar behavior was observed on coatings at different CS concentrations and electrodeposition times (data not shown).

3.2. Surface morphology

The SEM images in Figure 3 indicate the morphologies obtained by 0.1, 0.5, and 1.0% CS electrodeposition samples with 1.5 V at 2.5 min. It can be seen that the higher concentration of CS in the electrodeposition solution, the greater amount of CS particles on the surface. Figure 3d shows the fine CS particles that cover the entire surface with 1.0% CS electrodeposition. On the contrary, only a few particles spread on the electrodeposited sample with 0.1 and 0.5% CS (arrows) (Figure 3b and c).

When the voltage is increased to 3 V, important changes can be observed. Figure 4 shows the different morphologies obtained after 20 and 30 min of electrodeposition with three different CS concentrations. Compared to the blank sample (Figure 3a), it is easy to identify the chitosan deposit on the surfaces. There are fine CS particles forming when using chitosan concentrations of 0.1% and 0.5% in 20 min (arrows, Figures 4a and c). A thin, porous CS layer is built up with 1.0% CS at 20 min (Figure 4e). When the electrodeposition time is raised to 30 min for 0.1% to 0.5%

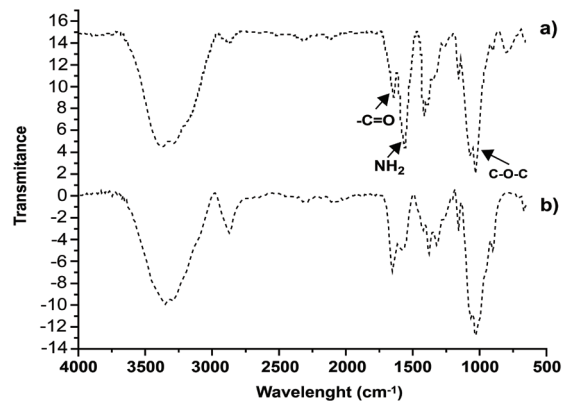


Figure 2. FTIR spectra of electrodeposited chitosan a) for 1.0% CS -30 min and b) native CS.

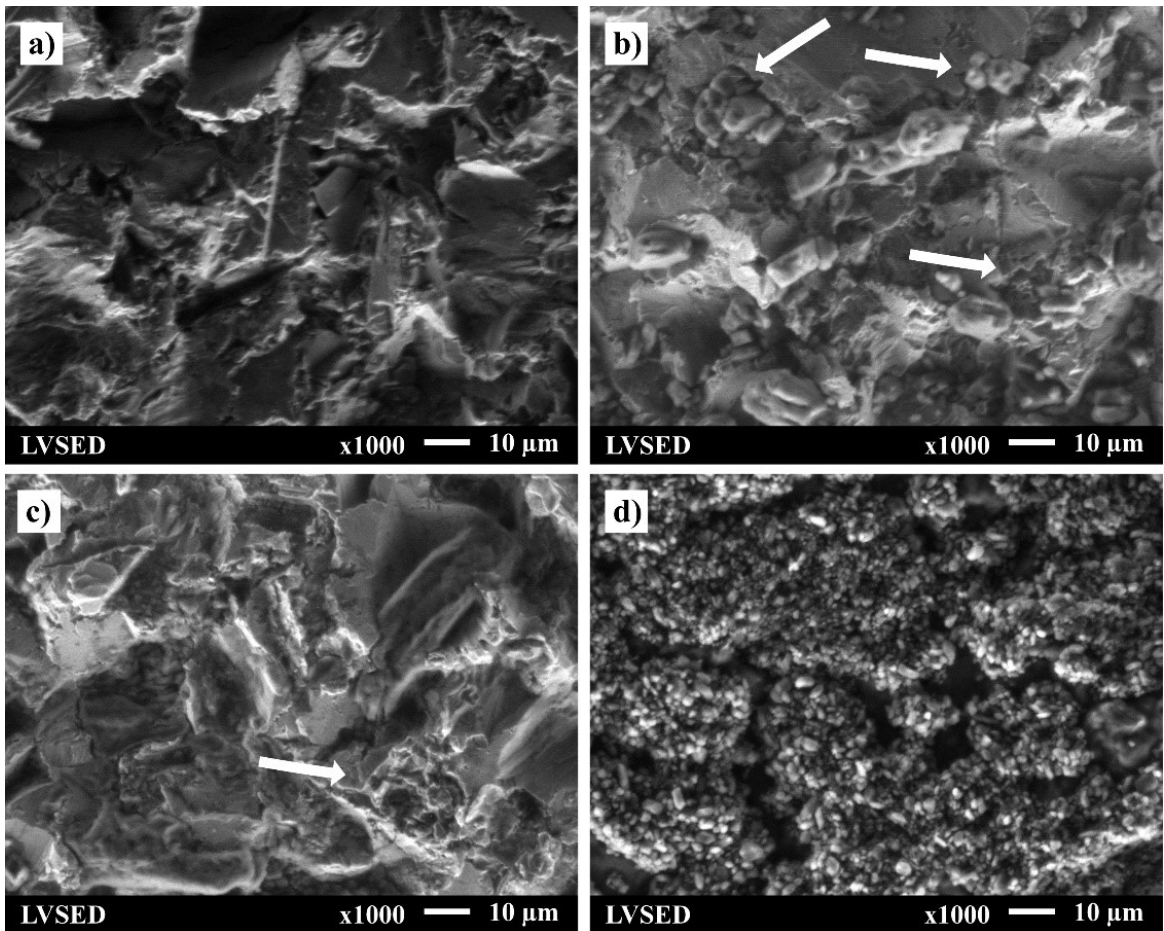


Figure 3. SEM micrographs at 1000x magnification of the Ti-6Al-4V surfaces electrodeposited with chitosan at 1.5 [V] and 2.5 min: a) blank sample; b) 0.1%CS; c) 0.5%CS and d) 1.0%CS. Calibration bar:10 µm.

CS (Figures 4b and d), there is an increase and accumulation of CS particles, and a non-uniform distribution. In contrast, increasing the electrodeposition time to 30 min, the 1.0% CS solution forms a thick, porous layer, uniformly distributed along the substrate surface (Figure 4f). This behavior can be explained by the fact that a low concentration of CS can reduce the amount of polymer chains near the substrate, and thereby only a few amines can be deprotonated to form a stable insoluble layer³⁵. Thus, the formation of continuous layers of chitosan can take place at higher CS concentrations and longer times.

In contrast to the electrodeposited samples, no visible changes are detected with the 1.0%CS adsorption samples (Figure 5). While electrodeposited samples were coated (Figures 4c through 4f), adsorption samples were not. Apparently, the contact only with the chitosan solution does not generate any interaction with the surface (Figure 5).

According to Liu et al.³², Ra et al.³³, Fernandes et al.³⁴, and Benea et al.³⁵, CS electrodeposition occurs due to a deprotonation of amine groups caused by the application of a certain current density. Nevertheless, when no current is applied (adsorption), this deprotonation does not take place, and the possibilities for CS deposition are significantly hindered.

As seen in Figures 4e and 4f, the 1.0%CS coating shows a highly porous morphology with a pore size of about 118 µm and 80 µm for 20 and 30 min electrodeposition, respectively (Figure 6). The pores are similar to the typical structure of pure CS hydrogel scaffolds, formed by charge interactions³⁷. Due to the fact that electrodeposition occurs through amine deprotonation and loss of solubility close to the surface, it is possible that at greater electrodeposition times, a higher number of molecules undergo these changes, thereby creating a denser structure with a consequent smaller pore size. Porosity is essential in prostheses coatings to facilitate cell migration and proliferation^{38,39}. Furthermore, pore size and structure would allow cell proliferation and a favorable arrangement of cells which is particularly convenient for biological applications^{37,38}. This porosity would also play an important role in the encapsulation and controlled release of drugs of interest, such as antibiotics and growth and differentiation factors^{40,41}. The 1.0% CS layer electrodeposited during 30 min shows an apparent high porosity (Figure 4f) compared to the layer electrodeposited during 20 min (Figure 4e). However, diameter values tended to be smaller for deposition time of 30 min of electrodeposition than 20 min. At higher CS concentrations, the viscosity of the solution increases, and thereby, the pore size decreases⁴². Additionally, in both times,

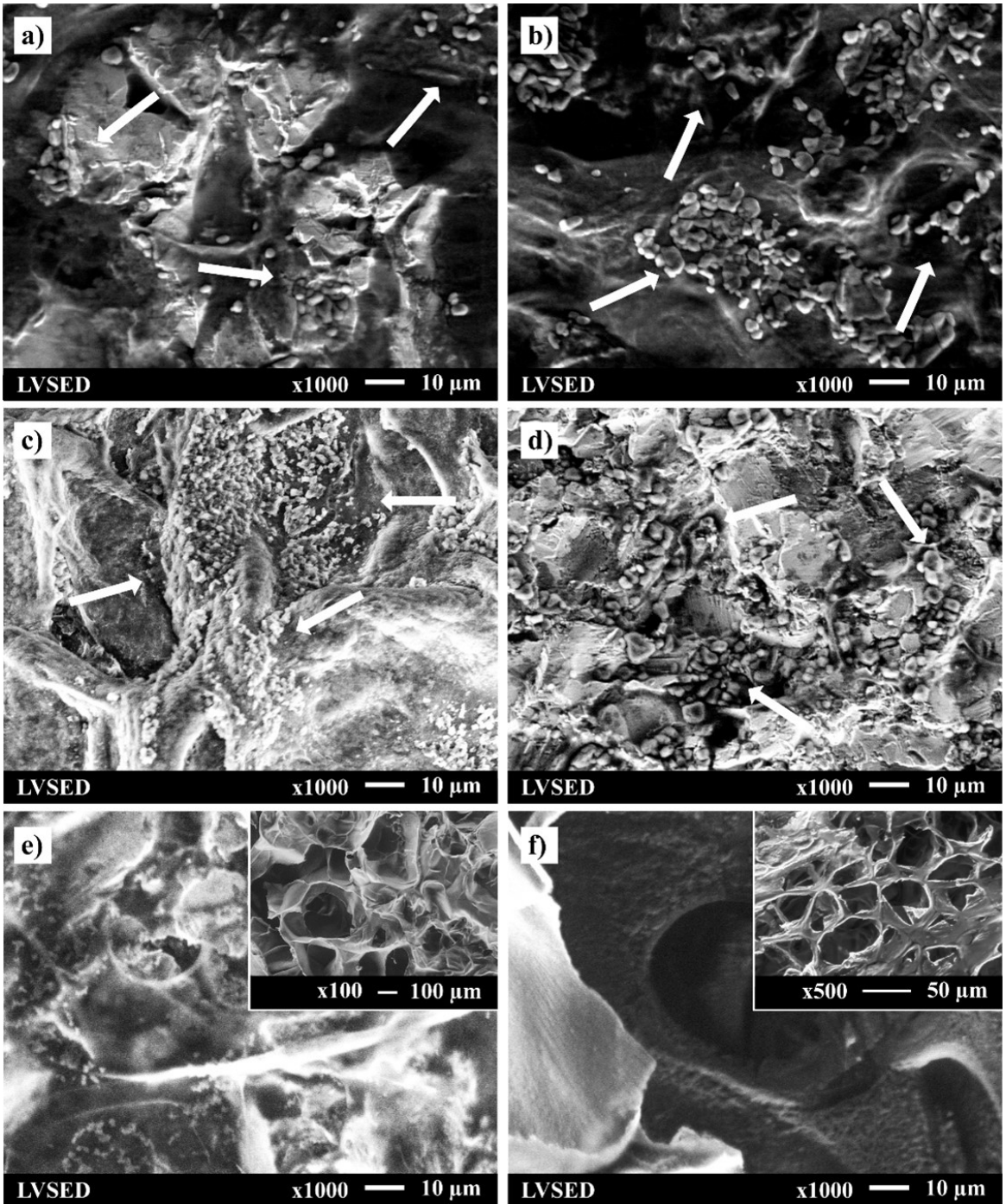


Figure 4. SEM micrographs at 1000x magnification of the surface electrodeposited with chitosan at 3[V]: a) 0.1%CS –20-min; b) 0.1%CS –30-min; c) 0.5%CS –20-min; d) 0.5%CS –30-min; e) 1.0%CS –20-min; f) 1.0%CS –30-min. Calibration bar:10 µm.

the CS coating had a broad size distribution (Figure 6). In general, the results suggest that the number of pores and size are time and CS concentration dependent.

Coating thickness was measured on the cross-sections of 1.0%CS samples at 20 and 30 min exposures. Figure 7 shows the cross-sections and the EDS analysis of CS coatings. It is observed that the electrodeposited coating with 20-min exposure

has a lower thickness than the coating with 30 min exposure. Measured thicknesses are in the range of 14.12 to 20.94 µm for the coatings with 20 min and between 36.09 to 70.72 µm for the coatings with 30 min. EDS maps show a high level of oxygen in the CS coatings (yellow color). The presence of oxygen is due to the fact that chitosan is composed of β -1 \rightarrow linked 2-acetamido-2-deoxy- β -D-glucopyranose and

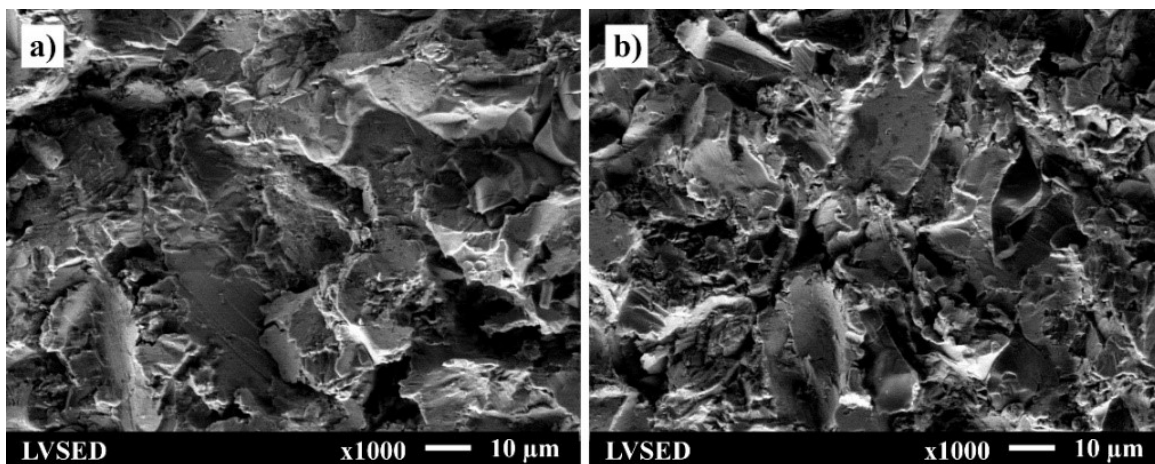


Figure 5. SEM micrographs at 1000x magnification of absorption samples with 1.0% CS at: a) 20 min, and b) 30 min. Calibration bar: 10 μm .

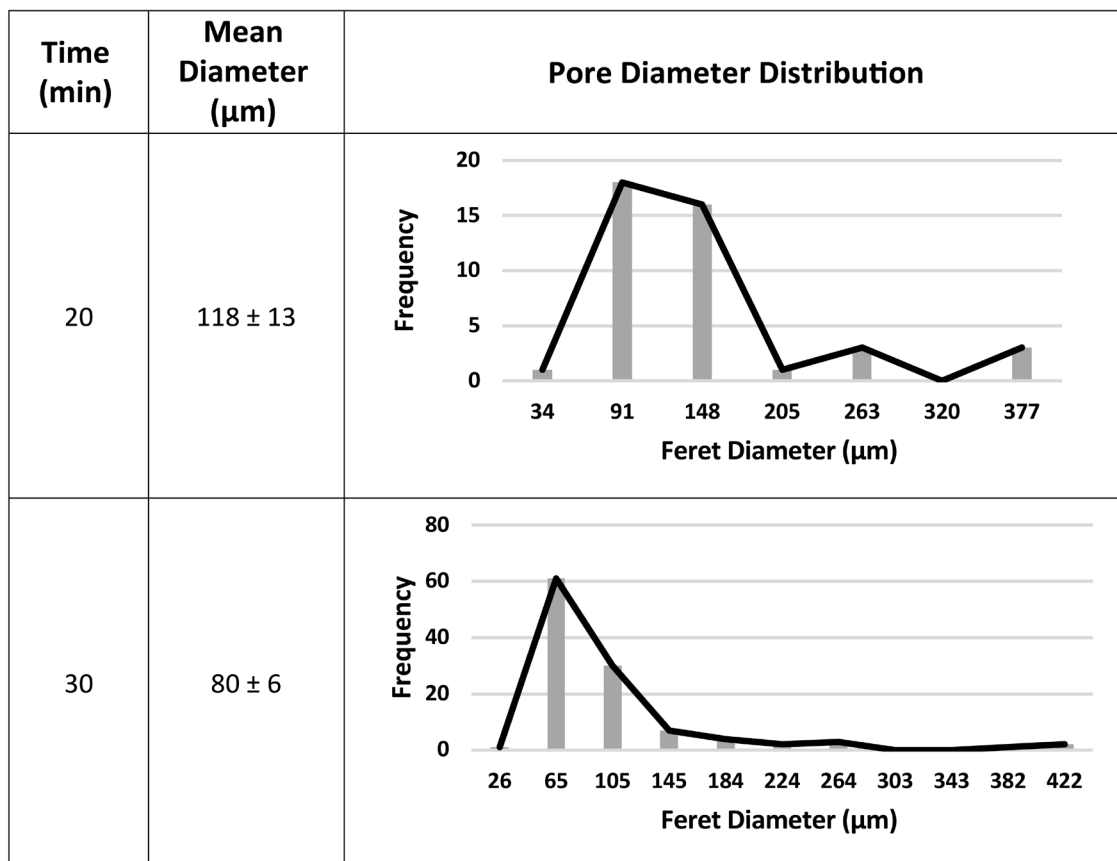


Figure 6. Pore diameter distribution of the electrodeposited chitosan coatings with 1.0% CS at 20 min and 30 min.

2-amino-2-deoxy-B-D-glucopyranose residues⁴³ which have a large amount of oxygen in their chains.

3.3. Assessment of coating adhesion

Using scratch testing, the effects of different electrodeposition conditions on coating adhesion to Ti-6Al-4V surfaces can be

studied. Figure 8 shows the friction coefficient versus normal force applied on coated samples of different concentrations compared to the blank samples. The coefficient of friction (COF) for the blank samples reached an average value of 0.45, while the coated samples of 1.0% CS-30 min and 1.0% CS-20 min that produced a continuous layer showed COF

lower than 0.3 at low loads. Only these two conditions are presented, provided that a more homogeneous coating was observed under SEM.

Two scenarios were identified. In the case of the 1.0% CS-30 min, the layer was present along the whole track of

the scratch test, decreasing the friction. In the case of the 1.0% CS-20 min, the layer was ploughed at about 17 N of load, exposing areas of Ti-6Al-4V to the indenter. In these samples, the COF increases up to about 0.4, which is characteristic of the blank samples.

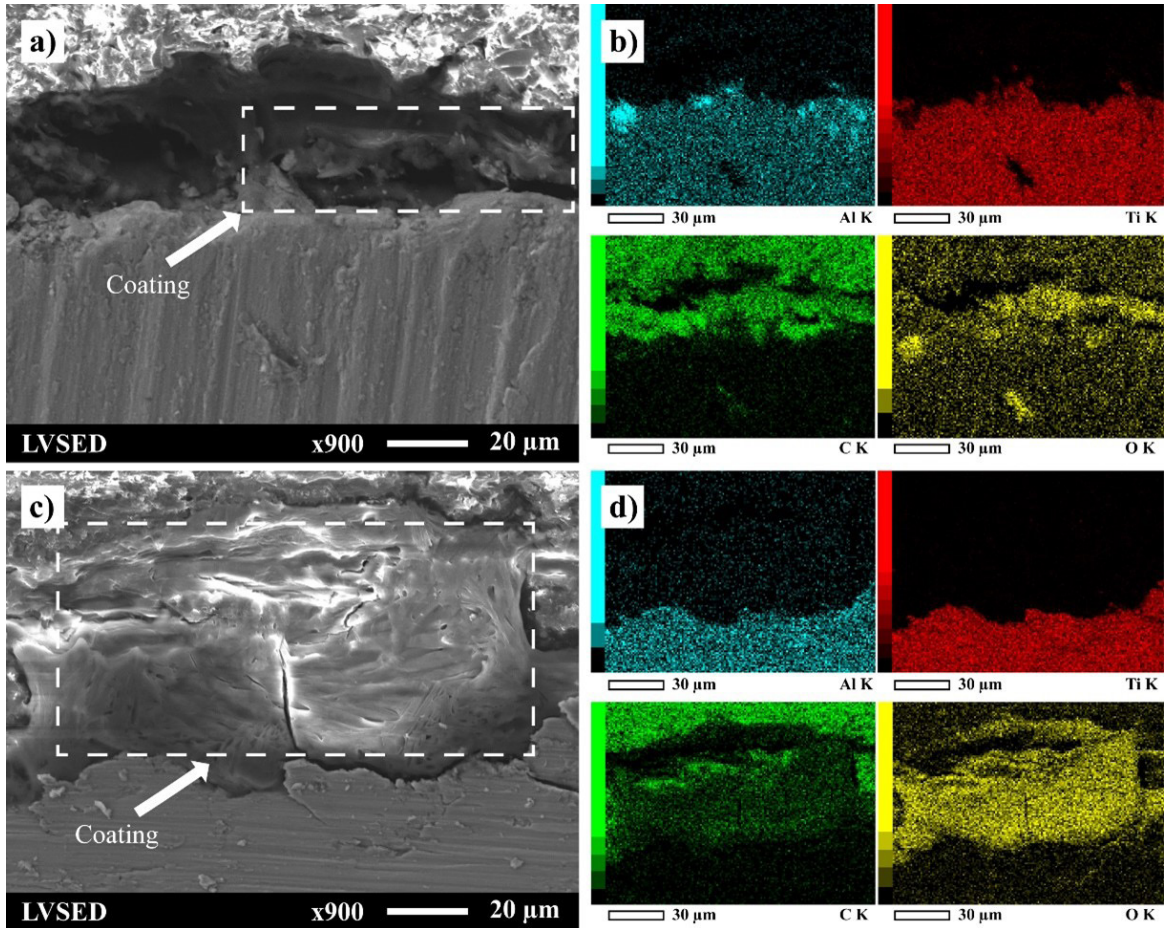


Figure 7. SEM micrographs at 900x magnification and EDS mapping (Al, Ti, C and O) of the cross sections for surfaces electrodeposited with 1.0% chitosan at 3 [V]: a) 1.0% CS-20 min micrograph, b) 1.0% CS-20 min mapping, c) 1.0% CS-30 min micrograph, d) 1.0% CS-30 min mapping. Calibration bar: 20 µm.

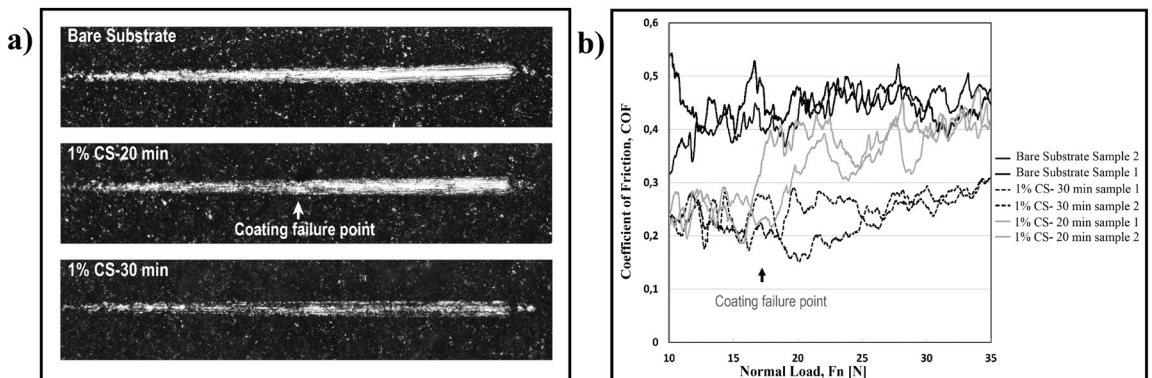


Figure 8. Scratch test results: a) Scratch tracks; b) Coefficient of friction as a function of the applied load for blank samples, 1%CS-30 min, and 1%CS-20 min samples.

It is worth noting that, under the conditions of the test, the indenter is producing plastic deformation over the Ti-6Al-4V surface, as predicted by Hertzian theory. This highlights the fact that the CS coatings demonstrated good adhesion for both samples:

- 1.0% CS-20 min sample failed at about 17 N, which denotes a failure at mean pressures beyond several GPa (GN/Indenter Contact Area) at the point of contact.
- 1.0% CS-30 min sample, at most scratches, did not fail by ploughing, which highlights that the coating was always present in between the indenter and the substrate.

The lower COF of coated samples compared to the blanks is an evidence that the stress applied could not induce its detachment but only a progressive plastic deformation of the substrate⁴⁴.

3.4. Coating stability

Swelling tests were performed at 37 °C, in PBS media, as a way to assess the hydrogel coating stability in physiological conditions. This methodology is commonly used to assess hydrogel stability⁴⁵. Furthermore, weight loss through swelling tests have been previously used to evaluate the stability of chitosan-vancomycin electrodeposited coatings⁴⁶. Figure 9 shows the swelling kinetics only for 1.0% CS coatings that formed a continuous hydrogel layer on the Ti-6Al-4V surface. Both coatings (formed after 20 min and 30 min) presented initially significantly high swelling degrees, but immediately they experienced a decrease in their swelling capacity. The 1.0% CS-30 min coating exhibited a slight swelling again after 3 h of testing. Although CS has available free hydroxyl and amino groups that could form strong hydrogen bonds^{31,47}, the deposited coatings do not retain moisture and degrade rapidly. This is probably due to CS intermolecular interactions, and a crosslinking agent, such as glutaraldehyde or genipin, would be needed to create a more stable structure⁴⁸. Another possibility is that the CS structure needs to be modified for an auto-crosslinking mechanism⁴⁵. Without a more robust crosslinking, as observed, the coating easily degrades in the presence of electrolytes in aqueous media (PBS); the low swelling degree values also corroborate this fact. In both cases, swelling equilibrium is reached after 3h. The coatings prepared after 30 min of electrodeposition showed higher swelling than the 20 min coatings, according to the statistical analysis.

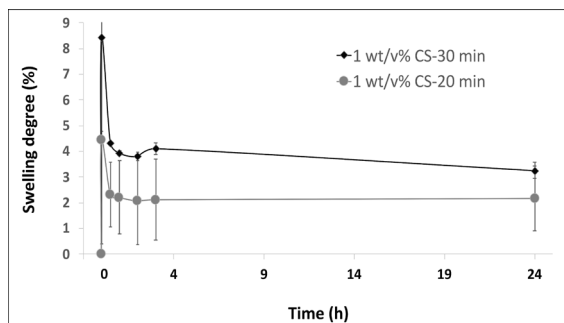


Figure 9. Swelling kinetics in PBS media for a 1.0% CS coating at two different electrodeposition times.

The overall assessment of process parameters of electrodeposition presented in this study indicates that the higher the CS concentration, higher voltage, and longer periods of time in electrodeposition assure a continuous thicker layer and full coverage of the Ti-6Al-4V. The longer the time of exposure increases the thickness and determines smaller micron-size pores on the CS surface. The pore-structure is of interest for cell proliferation and enhanced osseointegration. Further studies are planned for *in-vitro* cell-assays and evaluation of biocompatibility of the surfaces. Scratch results highlight a significantly high adhesion between the CS and the substrate. Although this assessment as presented is only qualitative, the technique proves to be sensitive to denote the continuous presence of the coating between the indenter and the substrate at high contact stresses. The swelling tests denote a rapid swelling of the electrodeposited CS. Further research will be carried out to improve this response. The CS by electrodeposition is a promising technique to deposit a highly biocompatible layer.

4. Conclusions

Chitosan coatings were successfully electrodeposited on Ti-6Al-4V substrates. CS deposition on Ti-6Al-4V is affected by polymer concentration, electrodeposition time, and voltage. Low concentrations of CS limit deprotonation and thereby the formation of a continuous insoluble film. Moreover, by examining the CS coating surface, it was determined that the homogeneity, thickness, and pore size are influenced by electrodeposition time. Likewise, the adhesion behavior is affected by the concentration and electrodeposition time. In the window of testing of this study, it was found that a coating with full coverage of the surface, with micron-size open porosity, and good adhesion is attained using higher voltage, higher CS concentration, and longer periods of electrodeposition time. Therefore, electrodeposition of CS coatings is feasible if these parameters are correctly controlled. Nevertheless, as evidenced by the swelling tests, these coatings lack stability in physiological conditions without using a proper crosslinking agent. Future studies to include CS crosslinking, and *in vitro* cell adhesion, proliferation, and differentiation tests will allow a complete understanding of the generated coatings.

5. Acknowledgements

This work was supported by Universidad San Francisco de Quito (Grant Number HUBI-16939). The authors are thankful to Centro de Ingeniería y Desarrollo Industrial, CIDESI -México for their valuable help in performing scratch tests.

6. References

1. Ödman, J, Lekholm U, Jemt T, Br nemark P-I, Thilander B. Osseointegrated titanium implants: a new approach in orthodontic treatment. *Eur J Orthod.* 1988;10(1):98-105. <http://dx.doi.org/10.1093/ejo/10.1.98>.
2. Guglielmotti MB, Olmedo DG, Cabrini RL. Research on implants and osseointegration. *Periodontol* 2000. 2019;79(1):178-89. <http://dx.doi.org/10.1111/prd.12254>.

3. Atallah R, Leijendekkers RA, Hoogbeem TJ, Frölke JP. Complications of bone-anchored prostheses for individuals with an extremity amputation: a systematic review. *PLoS One*. 2018;13(8):e0201821. <http://dx.doi.org/10.1371/journal.pone.0201821>.
4. Taylor TD. Prosthodontic problems and limitations associated with osseointegration. *J Prosthet Dent*. 1998;79(1):74-8. [http://dx.doi.org/10.1016/S0022-3913\(98\)70197-0](http://dx.doi.org/10.1016/S0022-3913(98)70197-0).
5. Zarb GA, Schmitt A. The longitudinal clinical effectiveness of osseointegrated dental implants: the Toronto study. Part III: problems and complications encountered. *J Prosthet Dent*. 1990;64(2):185-94. [http://dx.doi.org/10.1016/0022-3913\(90\)90177-E](http://dx.doi.org/10.1016/0022-3913(90)90177-E).
6. Gwam CU, Mistry JB, Mohamed NS, Thomas M, Bigart KC, Mont MA, et al. Current epidemiology of revision total hip arthroplasty in the United States: national inpatient sample 2009 to 2013. *J Arthroplasty*. 2017;32(7):2088-92. <http://dx.doi.org/10.1016/j.arth.2017.02.046>.
7. Davies JE. Understanding peri-implant endosseous healing. *J Dent Educ*. 2003;67(8):932-49. <http://dx.doi.org/10.1002/j.0022-0337.2003.67.8.tb03681.x>.
8. Kienapfel H, Sprey C, Wilke A, Griss P. Implant fixation by bone ingrowth. *J Arthroplasty*. 1999;14(3):355-68. [http://dx.doi.org/10.1016/S0883-5403\(99\)90063-3](http://dx.doi.org/10.1016/S0883-5403(99)90063-3).
9. Liu Y, Rath B, Tingart M, Eschweiler J. Role of implants surface modification in osseointegration: a systematic review. *J Biomed Mater Res A*. 2020;108(3):470-84. <http://dx.doi.org/10.1002/jbm.a.36829>.
10. de Jonge LT, Leeuwenburgh SCG, Wolke JGC, Jansen JA. Organic-inorganic surface modifications for titanium implant surfaces. *Pharm Res*. 2008;25(10):2357-69. <http://dx.doi.org/10.1007/s11095-008-9617-0>.
11. Rizzi G, Scrivani A, Fini M, Giardino R. Biomedical coatings to improve the tissue-biomaterial interface. *Int J Artif Organs*. 2004;27(8):649-57. <http://dx.doi.org/10.1177/039139880402700802>.
12. Zhang X, Zhang G, Zhang H, Li J, Yao X, Tang B. Surface immobilization of heparin and chitosan on titanium to improve hemocompatibility and antibacterial activities. *Colloids Surf B Biointerfaces*. 2018;172:338-45. <http://dx.doi.org/10.1016/j.colsurfb.2018.08.060>.
13. Shukla SK, Mishra AK, Arotiba OA, Mamba BB. Chitosan-based nanomaterials: a state-of-the-art review. *Int J Biol Macromol*. 2013;59:46-58. <http://dx.doi.org/10.1016/j.ijbiomac.2013.04.043>.
14. Liao YZ, Xin MH, Li MC, Su S. Preparation and characterization O-lauroyl chitosan/poly(L-lactic acid) blend membranes by solution-casting approach. *Chin Chem Lett*. 2007;18(2):213-6. <http://dx.doi.org/10.1016/j.ccl.2006.12.024>.
15. Milella E, Cosentino F, Licciulli A, Massaro C. Preparation and characterisation of titania/hydroxyapatite composite coatings obtained by sol-gel process. *Biomaterials*. 2001;22(11):1425-31. [http://dx.doi.org/10.1016/S0142-9612\(00\)00300-8](http://dx.doi.org/10.1016/S0142-9612(00)00300-8).
16. Yang C-C, Lin C-C, Yen S-K. Electrochemical deposition of vancomycin/chitosan composite on Ti alloy. *J Electrochem Soc*. 2011;158(12):E152. <http://dx.doi.org/10.1149/2.105112jes>.
17. Shukla A, Fang JC, Puranam S, Hammond PT. Release of vancomycin from multilayer coated absorbent gelatin sponges. *J Control Release*. 2012;157(1):64-71. <http://dx.doi.org/10.1016/j.jconrel.2011.09.062>.
18. Avcu E, Baştan FE, Abdullah HZ, Rehman MAU, Avcu YY, Boccaccini AR. Electrophoretic deposition of chitosan-based composite coatings for biomedical applications: a review. *Prog Mater Sci*. 2019;103:69-108. <http://dx.doi.org/10.1016/j.pmatsci.2019.01.001>.
19. Mitzi DB. Thin-film deposition of organic-inorganic hybrid materials. *Chem Mater*. 2001;13(10):3283-98. <http://dx.doi.org/10.1021/cm0101677>.
20. Li Y, Wu K, Zhitomirsky I. Electrodeposition of composite zinc oxide-chitosan films. *Colloids Surf A Physicochem Eng Asp*. 2010;356(1-3):63-70. <http://dx.doi.org/10.1016/j.colsurfa.2009.12.037>.
21. Stevanović M, Djošić M, Janković A, Nešović K, Kojić V, Stojanović J, et al. Assessing the bioactivity of gentamicin-preloaded hydroxyapatite/Chitosan composite coating on titanium substrate. *ACS Omega*. 2020;5(25):15433-45. <http://dx.doi.org/10.1021/acsomega.0c01583>.
22. Nancy D, Rajendran N. Vancomycin incorporated chitosan/gelatin coatings coupled with TiO₂-SrHAP surface modified cp-titanium for osteomyelitis treatment. *Int J Biol Macromol*. 2018;110:197-205. <http://dx.doi.org/10.1016/j.ijbiomac.2018.01.004>.
23. Stevanović M, Djošić M, Janković A, Kojić V, Vukašinić-Sekulić M, Stojanović J, et al. Antibacterial <sc>graphene-based</sc> hydroxyapatite/chitosan coating with gentamicin for potential applications in bone tissue engineering. *J Biomed Mater Res A*. 2020;108(11):2175-89. <http://dx.doi.org/10.1002/jbm.a.36974>.
24. Wu LQ, Gadre AP, Yi H, Kastantin MJ, Rubloff GW, Bentley WE, et al. Voltage-dependent assembly of the polysaccharide chitosan onto an electrode surface. *Langmuir*. 2002;18(22):8620-5. <http://dx.doi.org/10.1021/la020381p>.
25. Zangmeister RA, Park JJ, Rubloff GW, Tarlov MJ. Electrochemical study of chitosan films deposited from solution at reducing potentials. *Electrochim Acta*. 2006;51(25):5324-33. <http://dx.doi.org/10.1016/j.electacta.2006.02.003>.
26. Balza JC, Zujur D, Gil L, Subero R, Dominguez E, Delvasto P, et al. Sandblasting as a surface modification technique on titanium alloys for biomedical applications: abrasive particle behavior. *IOP Conf Series Mater Sci Eng*. 2013;45:012004. <http://dx.doi.org/10.1088/1757-899X/45/1/012004>.
27. Fang CH, Lin YW, Sun JS, Lin FH. The chitosan/tri-calcium phosphate bio-composite bone cement promotes better osteointegration: an in vitro and in vivo study. *J Orthop Surg Res*. 2019;14(1):1-9. <http://dx.doi.org/10.1186/s13018-019-1201-2>.
28. Liu J, Wang X, Wang T, Li D, Xi F, Wang J, et al. Functionalization of monolithic and porous three-dimensional graphene by one-step chitosan electrodeposition for enzymatic biosensor. *ACS Appl Mater Interfaces*. 2014;6(22):19997-20002. <http://dx.doi.org/10.1021/am505547f>.
29. Hao C, Ding L, Zhang X, Ju H. Biocompatible conductive architecture of carbon nanofiber-doped chitosan prepared with controllable electrodeposition for cytosensing. *Anal Chem*. 2007;79(12):4442-7. <http://dx.doi.org/10.1021/ac062344z>.
30. Pang X, Zhitomirsky I. Electrodeposition of composite hydroxyapatite-chitosan films. *Mater Chem Phys*. 2005;94(2-3):245-51. <http://dx.doi.org/10.1016/j.matchemphys.2005.04.040>.
31. Wang Z, Zhang X, Gu J, Yang H, Nie J, Ma G. Electrodeposition of alginate/chitosan layer-by-layer composite coatings on titanium substrates. *Carbohydr Polym*. 2014;103(1):38-45. <http://dx.doi.org/10.1016/j.carbpol.2013.12.007>.
32. Liu Y, Kim E, Ghodssi R, Rubloff GW, Culver JN, Bentley WE, et al. Biofabrication to build the biology-device interface. *Biofabrication*. 2010;2(2):022002. <http://dx.doi.org/10.1088/1758-5082/2/2/022002>.
33. Zangmeister RA, Park JJ, Rubloff GW, Tarlov MJ. Electrochemical study of chitosan films deposited from solution at reducing potentials. *Electrochim Acta*. 2006;51(25):5324-33. <http://dx.doi.org/10.1016/j.electacta.2006.02.003>.
34. Fernandes R, Wu LQ, Chen T, Yi H, Rubloff GW, Ghodssi R, et al. Electrochemically induced deposition of a polysaccharide hydrogel onto a patterned surface. *Langmuir*. 2003;19(10):4058-62. <http://dx.doi.org/10.1021/la027052h>.
35. Benea L, Celis JP. Reactivity of porous titanium oxide film and chitosan layer electrochemically formed on Ti-6Al-4V alloy in biological solution. *Surf Coat Tech*. 2018;354:145-52. <http://dx.doi.org/10.1016/j.surfcoat.2018.09.015>.
36. Zhu Q, Liang B, Cai Y, Cao Q, Tu T, Huang B, et al. Layer-by-layer chitosan-decorated pristine graphene on screen-printed

- electrodes by one-step electrodeposition for non-enzymatic hydrogen peroxide sensor. *Talanta*. 2018;190:70-7. <http://dx.doi.org/10.1016/j.talanta.2018.07.038>.
37. Liu M, Wu C, Jiao Y, Xiong S, Zhou C. Chitosan-halloysite nanotubes nanocomposite scaffolds for tissue engineering. *J Mater Chem B Mater Biol Med*. 2013;1(15):2078-89. <http://dx.doi.org/10.1039/c3tb20084a>.
 38. Bružauskaitė I, Bironaitė D, Bagdonas E, Bernotienė E. Scaffolds and cells for tissue regeneration: different scaffold pore sizes: different cell effects. *Cytotechnology*. 2016;68(3):355-69. <http://dx.doi.org/10.1007/s10616-015-9895-4>.
 39. Cai S-J, Li C-W, Weihs D, Wang G-J. Control of cell proliferation by a porous chitosan scaffold with multiple releasing capabilities. *Sci Technol Adv Mater*. 2017;18(1):987-96. <http://dx.doi.org/10.1080/14686996.2017.1406287>.
 40. Yang CC, Lin CC, Liao JW, Yen SK. Vancomycin-chitosan composite deposited on post porous hydroxyapatite coated Ti6Al4V implant for drug controlled release. *Mater Sci Eng C*. 2013;33(4):2203-12. <http://dx.doi.org/10.1016/j.msec.2013.01.038>.
 41. Xiao J, Zhu Y, Liu Y, Zeng Y, Xu F. A composite coating of calcium alginate and gelatin particles on Ti6Al4V implant for the delivery of water soluble drug. *J Biomed Mater Res B Appl Biomater*. 2009;89(2):543-50. <http://dx.doi.org/10.1002/jbm.b.31246>.
 42. Lin H-Y, Yeh C-T. Controlled release of pentoxifylline from porous chitosan-pectin scaffolds. *Drug Deliv*. 2010;17(5):313-21. <http://dx.doi.org/10.3109/10717541003713733>.
 43. Sacco P, Furlani F, de Marzo G, Marsich E, Paoletti S, Donati I. Concepts for developing physical gels of chitosan and of chitosan derivatives. *Gels*. 2018;4(3):67. <http://dx.doi.org/10.3390/gels4030067>.
 44. Renoud P, Toury B, Benayoun S, Attik G, Grosgeat B. Functionalization of titanium with chitosan via silanation: evaluation of biological and mechanical performances. *PLoS One*. 2012;7(7):e39367. <http://dx.doi.org/10.1371/journal.pone.0039367>.
 45. Zujur D, Moret J, Rodriguez D, Cruz L, Lira J, Gil L, et al. A novel photocrosslinkable and cytocompatible chitosan coating for Ti6Al4V surfaces. *J Appl Biomater Funct Mater*. 2015;13(3):210-9. <http://dx.doi.org/10.5301/jabfm.5000227>.
 46. Ordikhani F, Tamjid E, Simchi A. Characterization and antibacterial performance of electrodeposited chitosan-vancomycin composite coatings for prevention of implant-associated infections. *Mater Sci Eng C*. 2014;41:240-8. <http://dx.doi.org/10.1016/j.msec.2014.04.036>.
 47. Mishra SK, Kannan S. Development, mechanical evaluation and surface characteristics of chitosan/polyvinyl alcohol based polymer composite coatings on titanium metal. *J Mech Behav Biomed Mater*. 2014;40:314-24. <http://dx.doi.org/10.1016/j.jmbbm.2014.08.014>.
 48. Shariatnia Z, Jalali AM. Chitosan-based hydrogels: preparation, properties and applications. *Int J Biol Macromol*. 2018;115:194-220. <http://dx.doi.org/10.1016/j.ijbiomac.2018.04.034>.

Erratum: Electrodeposition of Chitosan on Ti-6Al-4V Surfaces: A Study of Process Parameters

In the article “Electrodeposition of Chitosan on Ti-6Al-4V Surfaces: A Study of Process Parameters”, with DOI: <https://doi.org/10.1590/1980-5373-MR-2021-0552>, published in Materials Research, 25:e20210552, on page 1, where it was written:

Marco León^a , **Doménica Alvarez^a**, **Alfredo Valarezo^a**, **Lorena Bejarano^a**, **Daniela Viteri^b**,

Astrid L. Giraldo-Betancur^c , **Juan Muñoz-Saldaña^c**, **Jose Alvarez-Barreto^{b*}** 

^aUniversidad San Francisco de Quito, Instituto de Investigación de Materiales, Departamento de Ingeniería Mecánica, Quito, Ecuador.

^bUniversidad San Francisco de Quito, Departamento de Ingeniería Química, Laboratorio de Biomateriales-IDEMA, Quito, Ecuador.

^cCONACYT-Centro de Investigación y de Estudios Avanzados del IPN, Querétaro, México.

Should read:

Marco León^a , **Doménica Alvarez^a**, **Alfredo Valarezo^a**, **M. Lorena Bejarano^a**, **Daniela Viteri^b**,

Astrid L. Giraldo-Betancur^c , **Juan Muñoz-Saldaña^d**, **Jose Alvarez-Barreto^{b*}** 

^aUniversidad San Francisco de Quito, Instituto de Investigación de Materiales, Departamento de Ingeniería Mecánica, Quito, Ecuador.

^bUniversidad San Francisco de Quito, Departamento de Ingeniería Química, Laboratorio de Biomateriales, Quito, Ecuador.

^cCONACYT-Centro de Investigación y de Estudios Avanzados del IPN, Querétaro, México.

^dCentro de Investigación y de Estudios Avanzados del IPN, Laboratorio Nacional de Proyección Térmica, CENAPROT Lib. Norponiente 2000, Fracc. Real de Juriquilla, 76230 Querétaro, Qro. México.